

Angular Diameter Distances in Clumpy Friedmann Universes

Kenji TOMITA

*Yukawa Institute for Theoretical Physics
Kyoto University, Kyoto 606-8502, Japan*

(Received April 6, 1998)

Solving null-geodesic equations, behavior of angular diameter distances is studied in inhomogeneous cosmological models, which are given by performing N -body simulations with the CDM spectrum. The distances depend on the separation angle θ of ray pairs, the mass m and the radius r_s of particles consisting of galaxies and dark matter balls, and cosmological model parameters. The calculated distances are compared with the Dyer-Roeder angular diameter distance with the clumpiness parameter α ($= 0 - 1$), and for each ray pair the corresponding α is determined. Shooting many ray pairs, we derive statistical quantities such as the average value ($\bar{\alpha}$), the dispersion (σ_α), and the distribution of α .

It is found in four cosmological models with $(\Omega_0, \lambda_0) = (1, 0), (0.2, 0), (0.4, 0), (0.2, 0.8)$ for the particle parameters $m \simeq 2 \times 10^{11} M_\odot$ and $r_s = (10 - 40)h^{-1}$ kpc that (1) $\bar{\alpha}$ is nearly equal to 1 or the Friedmann distance is best fitted, (2) σ_α decreases with the increase of the redshift z and radius r_s , (3) for $\theta \gg 1$ arcsec, σ_α is very small, but for $\theta < 1$ arcsec it is so large that the use of only the the Friedmann distance ($\alpha = 1$) may cause some errors for quantitative analysis of cosmological lensing, (4) the distribution of α is symmetric and asymmetric for $\sigma_\alpha < 0.5$ and > 0.8 , respectively, and (5) σ_α is smallest and largest in models with (1, 0) and (0.2, 0), respectively. The cosmological constant has the role of decreasing σ_α .

§1. Introduction

Recently many kinds of lens phenomena are observed in strong and weak forms of deformed images of quasars and galaxies due to lenses of galaxies, clusters of galaxies, and large-scale matter distribution. Lensing is being used as a new observational tool for remote dark objects.

For the analysis of such lens phenomena, angular diameter distances are often used because of their convenience, but their definition is not unique. The most representative ones are the Friedmann distance and Dyer-Roeder distance, which are given as the distances in the homogeneous and smooth matter distribution and the distance in low-density regions in the inhomogeneous matter distribution, respectively. ^{1), 2)} The behavior of these distances has been discussed in various papers. ^{3) - 6)} It is important to clarify which angular diameter distance is most appropriate in the observation of our Universe. This problem depends on the separation angles θ of ray pairs, the mass m and radius r_s of lens objects, like galaxies and dark matter balls, and cosmological model parameters (Ω_0, λ_0) .

In this paper we first use for this purpose the inhomogeneous models which were produced in previous papers, ^{7), 8)} using N -body simulations, and we then consider many ray pairs which are made by solving null-geodesic equations in the above

mentioned models and from which the average properties of the angular diameter distances are derived, taking into account the values of θ, m, r_s, Ω_0 and λ_0 . In §2 the behavior of the Dyer-Roeder angular diameter distance with the clumpiness parameter α in various background models is given explicitly. In §3 the angular diameter distances in inhomogeneous models produced by the numerical simulations are derived. By comparing those with the Dyer-Roeder angular diameter distance, the value of α for each ray pair is determined, and its statistical behavior is presented. In §4 concluding remarks are given.

§2. Dyer-Roeder angular diameter distance with the clumpiness parameter α

The Dyer-Roeder angular diameter distance $D_A(z)$ satisfies

$$\frac{d^2}{dv^2}D_A + \frac{3}{2}(1+z)^5\alpha\Omega_0 D_A = 0, \quad (2.1)$$

where α is the clumpiness parameter and v is the affine parameter.³⁾⁻⁶⁾ v is related to z by

$$dz/dv = (1+z)^2[(\Omega_0 z + 1)(1+z)^2 - \lambda_0 z(2+z)]^{1/2}. \quad (2.2)$$

The cases $\alpha = 0$ and 1 represent the limiting distances in the empty region and the Friedmann distance in the homogeneous region.

As we consider the rays received by an observer at the present epoch, we have the conditions

$$D_A(0) = 0, \quad (dD_A/dz)_{z=0} = c/H_0, \quad (2.3)$$

where H_0 ($= 100h \text{ km s}^{-1} \text{ Mpc}^{-1}$) is the Hubble constant.

Here we consider four models with $(\Omega_0, \lambda_0) = (1, 0), (0.1, 0), (0.2, 0)$ and $(0.2, 0.8)$. The above equations are easily solved in each model and we obtain the z -dependence of $D_A(z)$ for $\alpha = 0$ and 1 and the α -dependence of $D_A(z)$ for $z = 0.5, 1, \dots, 5$, which are shown in Figs. 1, 2 and Figs. 3 ~ 6, respectively. These dependences are used to interpret the results in the next section.

§3. Angular diameter distances in inhomogeneous models produced by N -body simulations

For the quantitative analysis of image deformation in the lensing phenomena, we treated in previous papers various clumpy Friedmann models (cf. Refs. 7) and 8), and also Refs. 9) and 10)). In the present paper we use the same models for the statistical analysis of the angular diameter distances. In them we considered inhomogeneities in periodic boxes including $N = 32^3$ particles, whose distribution was produced by performing the N -body simulation in the background models S, O1, O2, and L with $(\Omega_0, \lambda_0) = (1, 0), (0.2, 0), (0.4, 0)$, and $(0.2, 0.8)$, respectively. For the simulation we used Suto's tree code¹¹⁾ during the time interval $0 \leq z \leq 5$. The

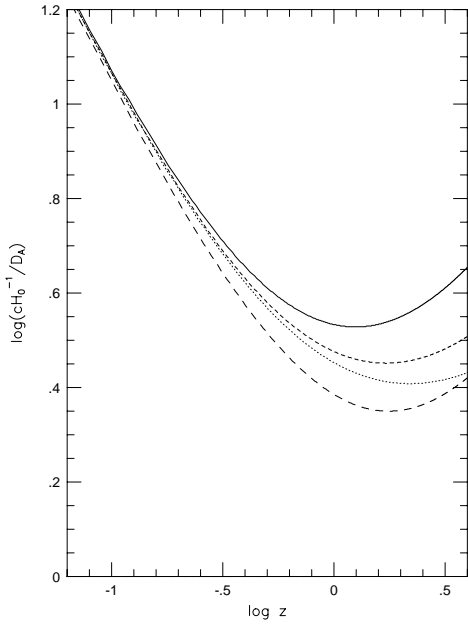


Fig. 1. The z dependence of the angular diameter distance D_A for $\alpha = 1$. Models S(1,0), O1(0.2,0), O2(0.4,0) and L(0.2,0.8) are denoted by solid, dotted, short dash, long dash lines, respectively.

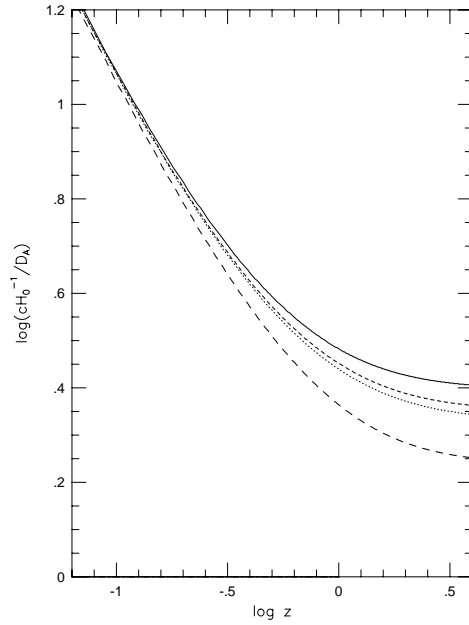


Fig. 2. The z dependence of the angular diameter distance D_A for $\alpha = 0$. Lines have the same meaning as in Fig. 1.

initial conditions were given in the CDM spectrum with the power $n = 1$ and the dispersion $\sigma_8 = 0.94$, using Bertschinger's software *COSMICS*,¹²⁾ where the Hubble parameter was specified as $h = 0.5, 0.7, 0.6$ and 0.7 for model S, O1, O2 and L, respectively.

The present sizes of the periodic boxes and the particle mass are

$$L_0 = (32.5, 50, 39.7, 50)h^{-1}\text{Mpc}, \quad (3.1)$$

and

$$m (= \rho_{B0}L_0^3/N) = (2.90, 2.11, 2.11, 2.11) \times 10^{11}h^{-1}M_\odot \quad (3.2)$$

for models S, O1, O2 and L, respectively, where $\rho_{B0} = 3H_0^2\Omega_0/(8\pi G)$.

In all models, particles consist of compact lens objects which are galaxies and dark matter balls with the same mass m and the same constant physical radius r_s . The representative value of r_s is $20h^{-1}$ kpc, but for comparison the cases of $r_s = 10h^{-1}$ kpc and $40h^{-1}$ kpc are also considered. In a previous paper⁷⁾ it was assumed that in model S particles consist of compact lens objects (20%) with $r_s = 20h^{-1}$ kpc and clouds (80%) with the same mass m and $r_s \geq 20h^{-1}$ kpc. In this paper we take the model S including only compact lens objects with various r_s . Model S with larger r_s corresponds effectively to the case including clouds with larger r_s .

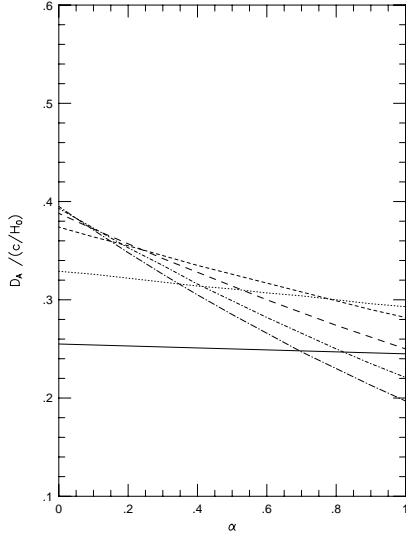


Fig. 3. The α dependence of the angular diameter distance D_A in the model S with $(\Omega_0, \lambda_0) = (1, 0)$. The epochs with $z = 0.5, 1, 2, 3, 4$, and 5 are denoted by solid, dotted, short dashed, long dashed lines, respectively.

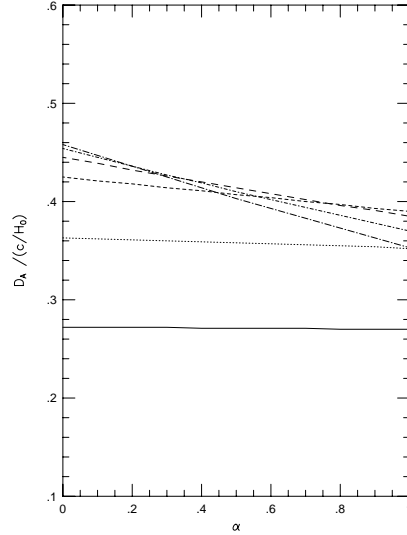


Fig. 4. The α dependence of the angular diameter distance D_A in the model O1 with $(0.2, 0)$. Lines have the same meaning as in Fig. 3.

The line-element of inhomogeneous models is expressed as

$$ds^2 = -(1 + 2\varphi/c^2)c^2 dt^2 + (1 - 2\varphi/c^2)a^2(t)(d\mathbf{x})^2/[1 + \frac{1}{4}K(\mathbf{x})^2]^2, \quad (3.3)$$

where φ is the gravitational potential connected with the matter distribution through the Poisson equation, and K is the signature (\pm or 0) of the spatial curvature. The physical radius r_s is expressed using the comoving radius x_s as $r_s = a(t)x_s$ and it is taken into consideration in the form of a softening parameter (r_s) in the gravitational force as $1/[a(t)(\mathbf{x} - \mathbf{x}_n)^2 + (r_s)^2]$, where \mathbf{x}_n is the position vector of n -th particle.

Let us consider a pair of rays received by the observer with the separation angle θ . By solving null-geodesic equations, which were obtained in the previous papers,^{7), 8)} the interval of the two rays at any epoch can be derived. If $(\Delta\mathbf{x})_\perp$ is the component of the deviation vector perpendicular to the central direction of the rays, the angular diameter distance D_A is defined as

$$D_A = a(t)(\Delta\mathbf{x})_\perp[1 + \frac{1}{4}K(\mathbf{x})^2]^{-1}/\theta, \quad (3.4)$$

where the factor $(1 - 2\varphi/c^2)$ is neglected, because $|\varphi/c^2| \ll 1$ locally. The above expression can be rewritten by use of $y^i (\equiv a_0 x^i / R_0)$ as

$$D_A = \frac{R_0}{(1+z)F}(\Delta\mathbf{y})_\perp/\theta, \quad (3.5)$$

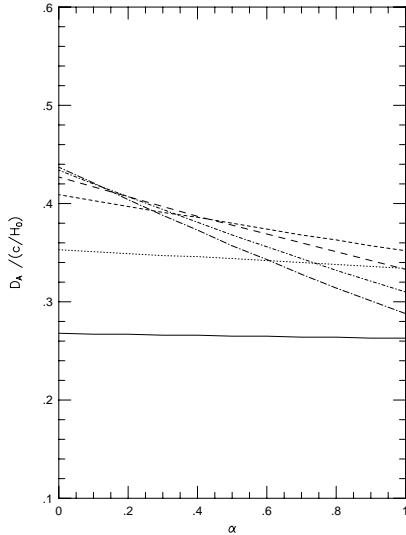


Fig. 5. The α dependence of the angular diameter distance D_A in the model O2 with (0.4, 0). Lines have the same meaning as in Fig. 3.

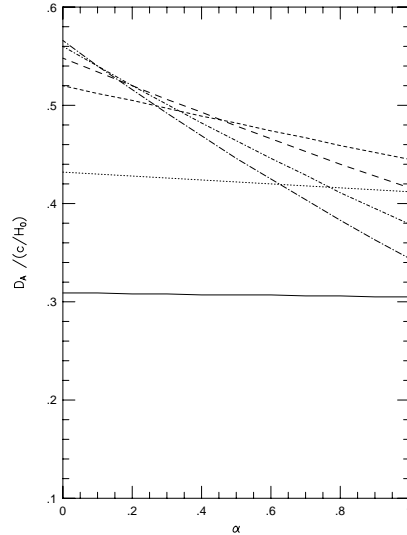


Fig. 6. The α dependence of the angular diameter distance D_A in the model L with (0.2, 0.8). Lines have the same meaning as in Fig. 3.

where $F \equiv 1 - \frac{1}{4}(R_0 H_0 / c)^2 (1 - \Omega_0 - \lambda_0)(\mathbf{y})^2$, $a_0 = a(t_0)$, and $R_0 \equiv L_0 / N^{1/3}$.

Behavior of the angular diameter distance depends on the separation angle θ . In the cosmological observation for angular sizes of compact radio sources by Kellerman,^{13),14)} it was found to be on the order of milli-arcseconds, or $\theta \sim 0.005$ arcsec. Accordingly we adopt $\theta = 0.005$ arcsec as a representative value and for comparison $\theta = 0.1$ and 20 arcsec as other representative values.

In the present lensing simulation we considered five parameter sets (r_s, θ) , A. ($20h^{-1}$ kpc, 0.005 arcsec), B. ($40h^{-1}$ kpc, 0.005 arcsec), C. ($10h^{-1}$ kpc, 0.005 arcsec), D. ($20h^{-1}$ kpc, 0.1 arcsec) and E. ($20h^{-1}$ kpc, 20 arcsec), and performed the ray-shooting of 500 ray pairs for each parameter set in the four models. At the six epochs $z = 0.5, 1, 2, 3, 4$ and 5, we compared the calculated distances with the Dyer-Roeder distance and determined the corresponding value of α . Since the angular diameter distance depends on α linearly for $0 \leq z \leq 5$, we define α as follows for the calculated distance D_A :

$$\alpha = (D_A - D_{DR}) / (D_F - D_{DR}), \quad (3-6)$$

where D_{DR} is the limiting Dyer-Roeder distance with $\alpha = 0$ and D_F is the calculated Friedmann distance in the homogeneous case. This D_F is equal to the Dyer-Roeder distance with $\alpha = 1$, except for small errors in numerical integrations.

As a result of statistical analysis for this ray-shooting, we derived the average clumpiness parameter $\bar{\alpha}$, the dispersion σ_α , and the distribution $(N(\alpha))$ of α . Here

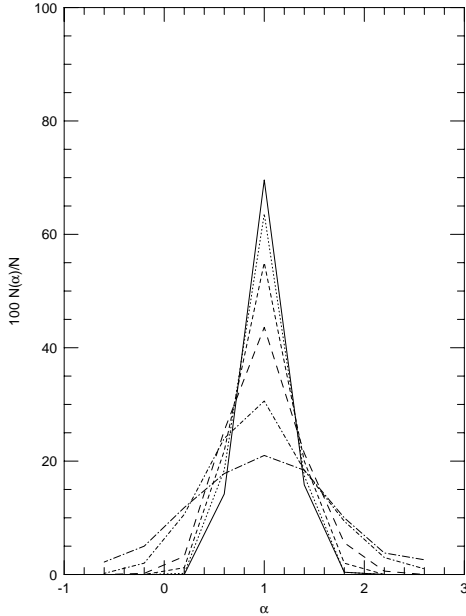


Fig. 7. The percentage ($100N(\alpha)/N$) of the distribution of α in bins with the interval $\Delta\alpha = 0.4$, for the parameter set A(20, 0.005) in model S with $(\Omega_0, \lambda_0) = (1.0, 0)$. Results for $z = 0.5, 1, 2, 3, 4, 5$ are denoted by dot-long dashed, dot-short dashed, long dashed, short dashed, dotted, solid lines, respectively

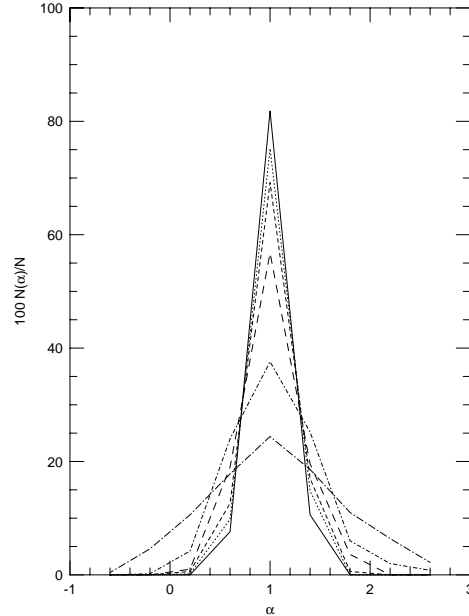


Fig. 8. The percentage ($100N(\alpha)/N$) of the distribution of α in bins with the interval $\Delta\alpha = 0.4$, for the parameter set B(40, 0.005) in model S with $(1.0, 0)$. Lines have the same meaning as in Fig. 7.

in order to study the frequency of ray pairs with α , we consider many bins with the interval $\Delta\alpha = 0.4$ and the centers $\alpha_i = 1.0 \pm 0.4i$ ($i = 0, 1, 2, \dots$). The number of ray pairs with $\alpha_i - \Delta\alpha/2 \leq \alpha \leq \alpha_i + \Delta\alpha/2$ is $N(\alpha_i)$ and the total number of ray pairs is $N(= \sum_i N(\alpha_i))$. In Tables I ~ IV we show $(\bar{\alpha}, \sigma_\alpha)$ for five parameter sets in model S, O1, O2 and L, respectively. In Figs. 7 ~ 18, we show the percentages of the distribution of α , that is, $100N(\alpha)/N$ for several parameter sets. The following types of statistical behavior are found from these tables and figures :

(1) $\bar{\alpha}$ is nearly equal to 1 in all models. However the individual values differ considerably from 1 for $\theta < 1$ arcsec, because the dispersion σ_α is large enough (for example $\sigma_\alpha \sim 0.5$ and 1 for $z = 1 - 2$ in model S and low-density models, respectively). Of the four models the dispersions are smallest and largest in models S and O1, respectively. Those in O2 and L are comparable. This situation is reflected also in the behaviors of the distribution of α , that is, around the point $\alpha = 1$ it is most symmetric and asymmetric in models S and O1, respectively.

(2) The dependence of σ_α on the radius of particles is large, σ_α decreases with an

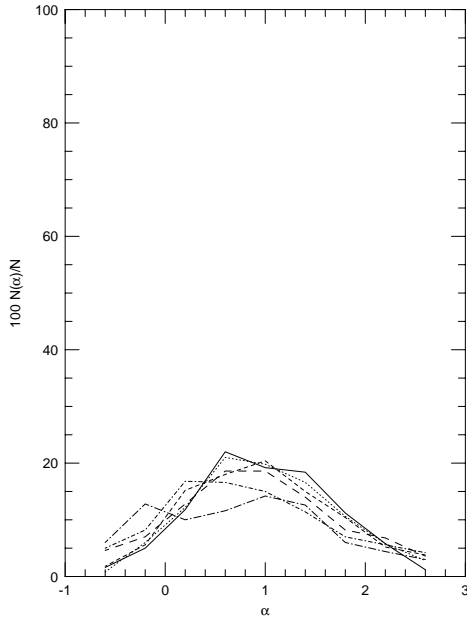


Fig. 9. The percentage ($100N(\alpha)/N$) of the distribution of α in bins with the interval $\Delta\alpha = 0.4$, for the parameter set A(20, 0.005) in model O1 with (0.2, 0). Lines have the same meaning as in Fig. 7.

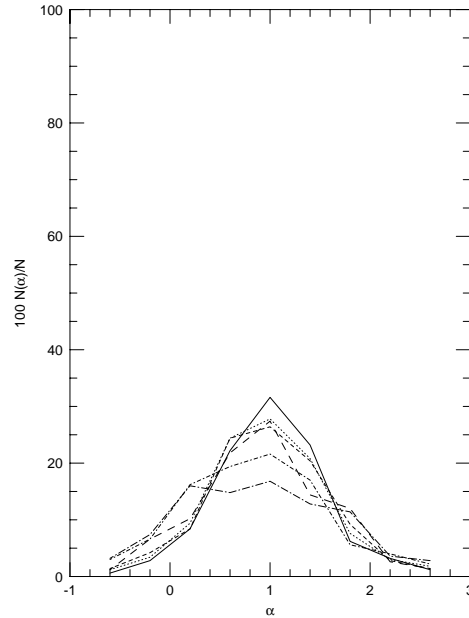


Fig. 10. The percentage ($100N(\alpha)/N$) of the distribution of α in bins with the interval $\Delta\alpha = 0.4$, for the parameter set B(40, 0.005) in model O1 with (0.2, 0). Lines have the same meaning as in Fig. 7.

increase of r_s , and when $r_s \ll 20h^{-1}\text{kpc}$, the dispersion σ_α is too large to determine $\bar{\alpha}$. The symmetry of the distribution of α increases in the order of C, A, and B (for the same θ) in all models. This is because with an increase of r_s the volume of empty regions included in the separation angles of ray pairs decreases and the inhomogeneous matter distribution in them is smoothed.

(3) With the increase of the redshift z , the dispersion σ_α decreases and the symmetry of the distribution increases in all models. This is because with an increase of z the number of particles included within the separation angles increases and the gravitational effect on ray pairs is homogenized.

(4) For $\theta \leq 1$ arcsec, the dependence of σ_α on the separation angle θ is small, as can be found by comparing columns A and D of the tables. In low-density models the dependence is rather large for $\theta \gg 1$ arcsec, as in column E. This is because in low-density models the quantity of matter included within the separation angle of ray pairs is much different in the cases of $\theta \leq 1$ and $\theta \gg 1$ arcsec, and the corresponding distance for $\theta \gg 1$ arcsec is clearly close to the Friedmann distance, in contrast to the case of $\theta \leq 1$ arcsec.

(5) In the case of $\sigma_\alpha \geq 0.8$, the distribution of α is irregular and asymmetric around $\alpha = 1$ and generally $N(\alpha)$ for $\alpha < 1$ is larger than that for $\alpha > 1$ (cf. Figs. 9 ~ 11,

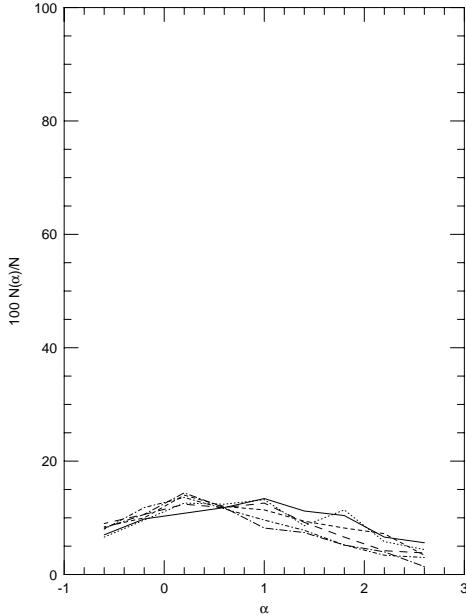


Fig. 11. The percentage ($100N(\alpha)/N$) of the distribution of α in bins with the interval $\Delta\alpha = 0.4$, for the parameter set C(10, 0.005) in model O1 with (0.2, 0). Lines have the same meaning as in Fig. 7.

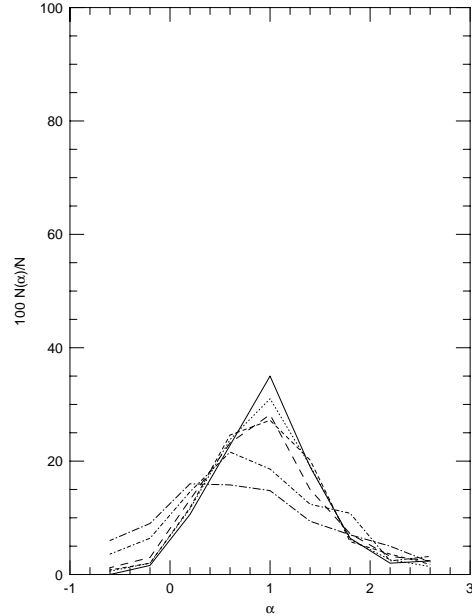


Fig. 12. The percentage ($100N(\alpha)/N$) of the distribution of α in bins with the interval $\Delta\alpha = 0.4$, for the parameter set E(20, 20) in model O1 with (0.2, 0). Lines have the same meaning as in Fig. 7.

13 ~ 17). This behavior suggests that the distribution function of α is not Gaussian in these cases. For ray pairs with $\sigma_\alpha \geq 0.8$, the z dependence of $\bar{\alpha}$ also is irregular and may decrease slightly from 1 with an increase of z . For ray pairs with $\sigma_\alpha < 0.5$, however, $\bar{\alpha}$ clearly approaches 1 with an increase of z .

(6) A positive cosmological constant has the role of decreasing σ_α and the asymmetry of the distribution of α (cf. Figs. 9 ~ 12 and Figs. 15 ~ 18).

Figures 3 ~ 6 in the previous section show for $z \sim 0.5$ that the change in the Dyer-Roeder distance (D_A) for the interval $\alpha = 0 \sim 1$ is very small. Accordingly, we can approximately use D_A with $\alpha = 1$ for $z \sim 0.5$, even if σ_α is larger than 1. For $z > 1$ and $\theta < 1$ arcsec, however, the change in D_A for this interval of α is not so small that the large dispersion (σ_α) brings a considerable fluctuation in the value of D_A . This means that for $z > 1$ and $\theta < 1$ arcsec, the realistic distance may deviate considerably from the Friedmann distance in low-density models.

§4. Concluding remarks

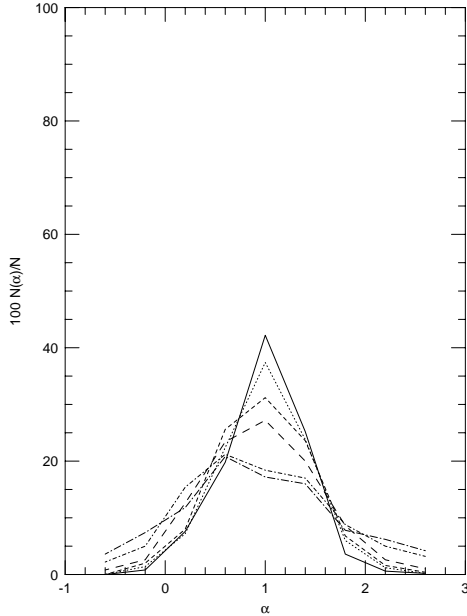


Fig. 13. The percentage ($100N(\alpha)/N$) of the distribution of α in bins with the interval $\Delta\alpha = 0.4$, for the parameter set A(20, 0.005) in model O2 with (0.4, 0). Lines have the same meaning as in Fig. 7.

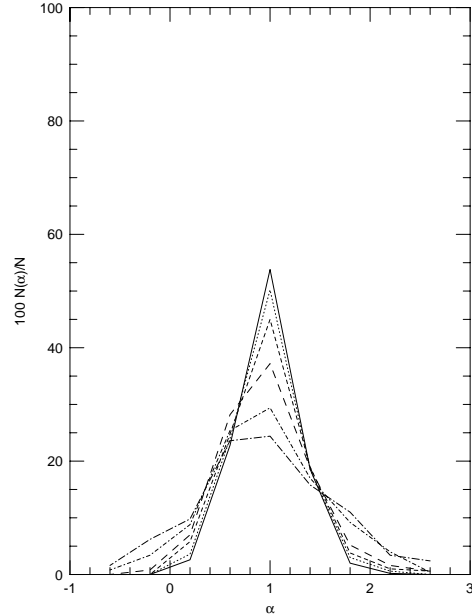


Fig. 14. The percentage ($100N(\alpha)/N$) of the distribution of α in bins with the interval $\Delta\alpha = 0.4$, for the parameter set B(40, 0.005) in model O2 with (0.4, 0). Lines have the same meaning as in Fig. 7.

Table I. The average clumpiness parameter $\bar{\alpha}$ and its dispersion σ_α in model S with $(\Omega_0, \lambda_0) = (1.0, 0)$. Columns A, B, C, D and E correspond to the parameter sets (20, 0.005), (40, 0.005), (10, 0.005), (20, 0.1) and (20, 20), respectively.

	A		B		C		D		E	
z	$\bar{\alpha}$	σ_α	$\bar{\alpha}$	σ_α	$\bar{\alpha}$	σ_α	$\bar{\alpha}$	σ_α	$\bar{\alpha}$	σ_α
0.5	1.07	0.93	1.12	0.78	1.01	1.31	1.08	0.84	1.06	0.76
1	1.01	0.57	1.05	0.43	0.98	0.81	1.02	0.50	1.01	0.40
2	1.01	0.36	1.02	0.28	0.99	0.54	1.01	0.33	1.00	0.26
3	1.00	0.27	1.02	0.21	0.99	0.42	1.01	0.25	1.00	0.19
4	1.00	0.23	1.01	0.18	0.99	0.35	1.01	0.21	1.00	0.16
5	1.00	0.20	1.01	0.16	0.99	0.30	1.00	0.18	1.00	0.14

By numerical ray-shooting in the N -body-simulating clumpy cosmological models, we studied the statistical behavior of the angular diameter distance D_A and determined the clumpiness parameter α by comparing it with the Friedmann distance ($\alpha = 1$) and the Dyer-Roeder distance ($\alpha > 0$). The results show that the average value of α is nearly equal to 1 and the dispersion (σ_α) decreases with an increase of z , but that for $\theta < 1$ arcsec, σ_α is ~ 0.5 in model S and ~ 1 in low-density models for $z = 1 - 2$. Hence the influence of the clumpiness is not small, because the

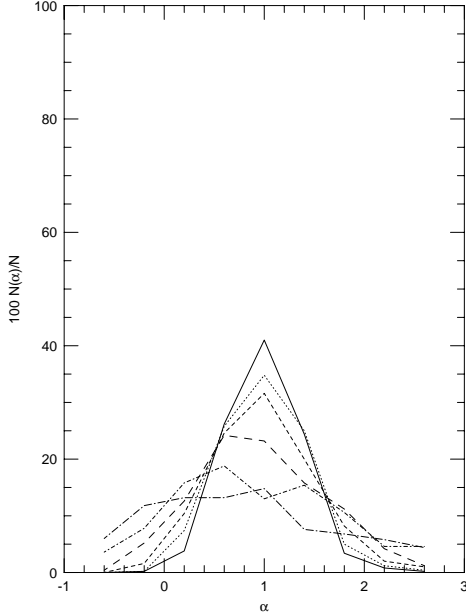


Fig. 15. The percentage ($100N(\alpha)/N$) of the distribution of α in bins with the interval $\Delta\alpha = 0.4$, for the parameter set A(20, 0.005) in model L with (0.2, 0.8). Lines have the same meaning as in Fig. 7.

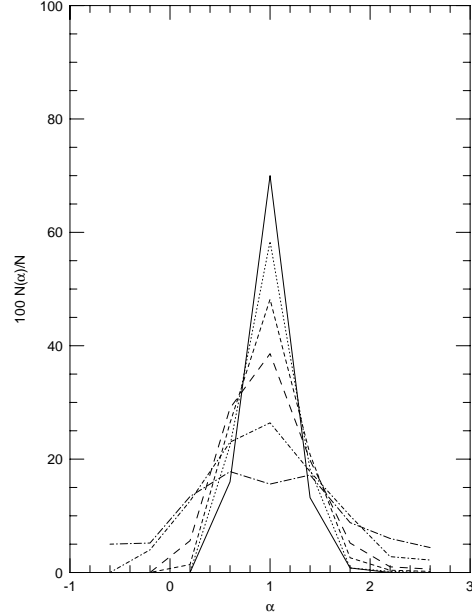


Fig. 16. The percentage ($100N(\alpha)/N$) of the distribution of α in bins with the interval $\Delta\alpha = 0.4$, for the parameter set B(40, 0.005) in model L with (0.2, 0.8). Lines have the same meaning as in Fig. 7.

Table II. The average clumpiness parameter $\bar{\alpha}$ and its dispersion σ_α in model O1 with (0.2, 0).

z	A		B		C		D		E	
	$\bar{\alpha}$	σ_α	$\bar{\alpha}$	σ_α	$\bar{\alpha}$	σ_α	$\bar{\alpha}$	σ_α	$\bar{\alpha}$	σ_α
0.5	1.01	2.42	1.23	1.28	1.07	4.08	0.99	2.39	0.91	1.48
1	0.94	1.43	1.05	0.86	0.91	2.38	0.93	1.42	0.96	1.08
2	1.00	1.03	1.02	0.73	0.95	1.63	0.99	0.99	1.00	0.78
3	0.98	0.89	1.01	0.63	0.95	1.37	0.99	0.87	1.00	0.66
4	0.98	0.85	0.99	0.59	0.93	1.31	0.98	0.83	1.00	0.60
5	0.96	0.80	0.97	0.55	0.89	1.26	0.97	0.78	1.00	0.54

difference between distances with $\alpha = 0$ and 1 is not small for $z > 1$. For $\theta \gg 1$ arcsec, σ_α is so small that the distance can be regarded approximately as the Friedmann distance. Therefore we can conclude for $\theta < 1$ arcsec that for rough or qualitative estimates of the lensing effect we can use the Friedmann angular diameter distance ($\alpha = 1$), but for the quantitative analysis of cosmological gravitational lensing, some errors may result from using only it at the high-redshift stage ($z > 1$).

For the behavior of the distribution ($N(\alpha)$), we found that when $\sigma_\alpha < 0.5$, $N(\alpha)$ is symmetric around $\alpha = 1$, and when $\sigma_\alpha \geq 0.8$, $N(\alpha)$ is irregular, and the symmetry is largest and smallest for S and O1 models, respectively.

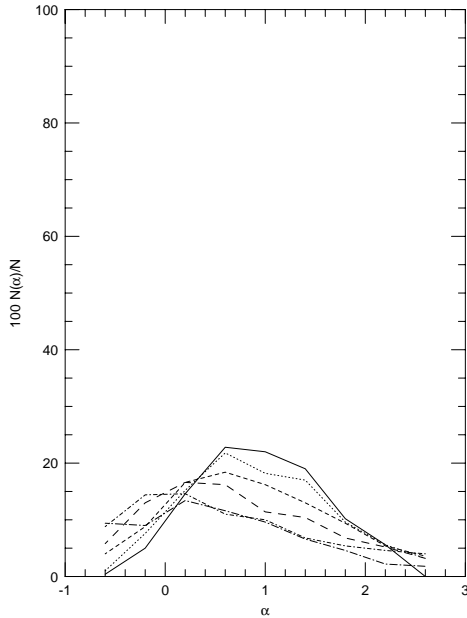


Fig. 17. The percentage ($100N(\alpha)/N$) of the distribution of α in bins with the interval $\Delta\alpha = 0.4$, for the parameter set C(10, 0.005) in model L with (0.2, 0.8). Lines have the same meaning as in Fig. 7.

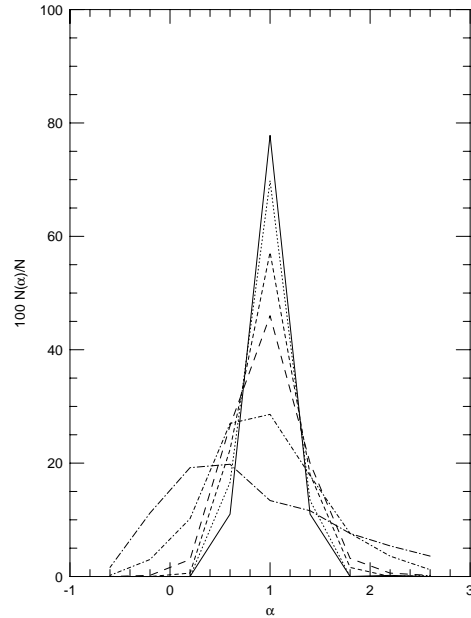


Fig. 18. The percentage ($100N(\alpha)/N$) of the distribution of α in bins with the interval $\Delta\alpha = 0.4$, for the parameter set E(20, 20) in model L with (0.2, 0.8). Lines have the same meaning as in Fig. 7.

Table III. The average clumpiness parameter $\bar{\alpha}$ and its dispersion σ_α in model O2 with (0.4, 0).

z	A		B		C		D		E	
	$\bar{\alpha}$	σ_α	$\bar{\alpha}$	σ_α	$\bar{\alpha}$	σ_α	$\bar{\alpha}$	σ_α	$\bar{\alpha}$	σ_α
0.5	1.00	1.01	1.00	0.79	0.99	1.71	1.00	0.97	1.00	0.86
1	1.02	0.89	1.00	0.65	1.03	1.50	1.01	0.86	1.00	0.65
2	0.99	0.62	0.98	0.46	1.01	1.01	0.99	0.60	0.98	0.43
3	0.99	0.51	0.99	0.37	0.99	0.80	1.00	0.50	0.99	0.34
4	0.99	0.45	0.99	0.32	0.97	0.68	0.99	0.44	0.99	0.30
5	0.99	0.40	0.99	0.29	0.97	0.63	0.99	0.38	0.99	0.27

In the present cosmological models all particles were assumed to be lens objects with equal masses and radii. As the number density of particles is larger than that of visible standard galaxies, most particles are regarded as invisible galaxies or dark matter balls. It is a crucial problem in cosmological lensing to specify how strong lenses these invisible objects are. If the particles corresponding to only visible galaxies are regarded as lens objects, σ_α may be smaller than that in the above case A. If all visible galaxies are lens objects with $r_s = 20h^{-1}$ kpc and the other particles are weaker lenses with $r_s \simeq 40h^{-1}$ kpc, the resultant values for $\bar{\alpha}$ and σ_α are between those in cases A and B.

Table IV. The average clumpiness parameter $\bar{\alpha}$ and its dispersion σ_α in model L with (0.2, 0.8).

z	A		B		C		D		E	
	$\bar{\alpha}$	σ_α	$\bar{\alpha}$	σ_α	$\bar{\alpha}$	σ_α	$\bar{\alpha}$	σ_α	$\bar{\alpha}$	σ_α
0.5	1.01	1.44	1.03	1.03	1.00	2.49	1.02	1.35	0.97	1.08
1	1.01	1.01	1.01	0.64	0.95	1.78	1.02	0.96	0.99	0.60
2	1.00	0.71	1.00	0.42	0.94	1.23	1.00	0.68	0.99	0.36
3	1.00	0.53	1.00	0.31	0.96	0.92	1.00	0.51	0.99	0.26
4	1.00	0.42	1.00	0.25	0.95	0.73	1.00	0.41	0.99	0.21
5	1.00	0.36	1.00	0.21	0.95	0.63	1.00	0.35	0.99	0.17

In the above averaging process, all light rays were taken into account. If we consider only weakly deflected light rays as contributing to weak lensing, the dispersion σ_α will be a slightly smaller than the values in the above tables. However, the contribution of strong lensing to σ_α is small because of its small frequency.

In this paper we treated the case in which m is on the order of the standard galaxy. If m is on the order of the rich-cluster mass, the influence of lensing on the distance is of course much larger and gives much larger dispersions. However, this situation is unrealistic.

Acknowledgements

The author would like to thank Y. Suto for helpful discussions about N -body simulations and referees for valuable suggestions. Numerical computations were performed on the YITP computer system.

References

- 1) C.C. Dyer and R.C. Roeder, *Astrophys. J.* **174** (1972), L115.
- 2) C.C. Dyer and R.C. Roeder, *Astrophys. J.* **189** (1974), 189, 167.
- 3) M. Kasai, T. Futamase, and F. Takahara, *Phys. Lett.* **A147** (1990), 97.
- 4) K. Watanabe and K. Tomita, *Astrophys. J.* **355** (1990), 1.
- 5) H. Asada, *Astro-ph/9803004*.
- 6) P. Schneider, J. Ehlers and E. E. Falco, *Gravitational Lenses* (Springer-Verlag, New York, 1992), p. 157.
- 7) K. Tomita, *Prog. Theor. Phys.* **99** (1989), 97.
- 8) K. Tomita, *Astro-ph/9806003*.
- 9) K. Tomita and K. Watanabe, *Prog. Theor. Phys.* **82** (1989), 563.
- 10) K. Tomita and K. Watanabe, *Prog. Theor. Phys.* **83** (1990), 467.
- 11) Y. Suto, *Prog. Theor. Phys.* **90** (1993), 1173.
- 12) E. Bertschinger, *Astro-ph/9506070*.
- 13) K.I. Kellermann, *Nature* **361** (1993), 134.
- 14) J.C. Jackson and M. Dodgson, *Mon. Not. R. Astron. Soc.* **278** (1996), 603.